Journal of the Korean Electrochemical Society
Vol. 2, No. 4, 1999, 202-208

Conditioning Effects on LSM-YSZ Cathodes for Thin-film SOFCs

You-Kee Lee† and Steven J. Visco*

Dept. of Semiconductor Engineering, Uiduk University, Kyongju 780-713, Korea
**Materials Sciences Division, Lawrence Berkeley National Laboratory, CA 94720, USA*
(Received August 12, 1999 : Accepted September 27, 1999)

Abstract

Composite cathodes of 50/50 vol% LSM-YSZ ($La_{1-x}Sr_xMnO_3$-yttria stabilized zirconia) were deposited onto dense YSZ electrolytes by colloidal deposition technique. The cathode characteristics were then examined by scanning electron microscopy (SEM) and studied by ac-impedance spectroscopy (IS). The conditioning effects on LSM-YSZ cathodes were seen and remedies for these effects were noted in order to improve the performance of a solid oxide fuel cell (SOFC). The effects of temperature on impedance, surface contamination on cathode bonding to YSZ electrolyte, changing Pt paste, aerosol spray technique applied to curved surface on microstructure and cell to cell variability were solved by testing at 900°C, sanding the YSZ surface, using only one batch of Pt paste, using flat YSZ plates and using consistent procedures and techniques, respectively. And then, reproducible impedance spectra were confirmed by using the improved cell and the typical spectra measured for an (air)LSM-YSZ/YSZ/LSM-YSZ(air) cell at 900°C were composed of two depressed arcs. Impedance characteristics of the LSM-YSZ cathodes were also affected by experimental conditions such as catalytic interlayer, composite cathode compositions and applied current.

초 록 : 50/50 vol% LSM-YSZ의 양극은 콜로이드 증착법에 의해 YSZ 전해질상에 증착하였다. 양극 특성은 주사 전자현미경과 임피던스 분석기에 의해 고찰하였다. LSM-YSZ 양극의 제조 조건에 따른 영향을 관찰하였으며, 그 영향에 대한 개선책이 고체산화물 연료전지의 성능향상을 위해 제시되었다. 임피던스에 대한 온도, YSZ 전해질로의 양극 접착에 대한 표면 오염, 사용하는 Pt 페이스트, 미세구조에 대한 곡표면에 가해진 연무질 분사기술과 셀과 셀의 변동성에 대한 영향들은 각각 900°C 측정, YSZ 표면 연마, 일단의 Pt 페이스트 사용, 평편한 YSZ 판의 사용과 일관된 절차와 기술의 사용에 의해 해결되었다. 이때 재현성있는 임피던스 스펙트럼들이 향상된 셀을 사용함으로써 얻어졌고, 900°C에서 (공기)LSM-YSZ/YSZ/LSM-YSZ(공기) 셀에 대해 측정된 전형적인 임피던스 스펙트럼들은 2개의 불완전한 호로 구성되었다. 또한 LSM-YSZ 양극의 임피던스 특성은 촉매층, 양극 조성, 인가 전류 등과 같은 실험 조건들에 의해서도 영향을 받았다.

Key words : LSM-YSZ, Colloidal deposition technique, Conditioning effects, Impedance characteristics

1. Introduction

In recent years several groups worldwide have been involved in the development of solid oxide fuel cells (SOFCs) capable of delivering high power at reduced temperatures and remarkable progress has been achieved in developing reduced temperature SOFCs. The approaches generally fall into two categories: the use of materials with substantially higher conductivity and/or fabrication of SOFCs using thin-film electrolyte membranes. Among the SOFCs the several methods for depositing thin-film onto porous electrodes/substrates have attracted widespread attention because the electrolyte ohmic loss was negligibly small, as electrolyte thickness was reduced.[1-6] We also developed a planar thin-film SOFC using a colloidal solution of YSZ deposited on porous electrode.[5] Clearly, after the resistance of the electrolyte has been lowered to acceptable (or negligible) levels, the performance of the anode and cathode becomes the limiting factor to performance at reduced temperatures. In our experience the performance of the nickel-yttria stabilized zirconia (Ni-YSZ) anode in thin-film SOFCs is excellent over a broad temperature range. However, the cathode overpotential can be limiting, particularly at temperature below 800°C.

$La_{1-x}Sr_xMnO_3$ (LSM) has been considered one of the most promising cathode materials for SOFC due to the good performance characteristics.[7] But at reduced temperatures (700~800°C), the related cathode overpotential is still large in SOFC. Therefore, it is necessary to further decrease the overpotential for LSM cathode. In recent studies, improvement of electrochemical performance relative to the performance of the conventional LSM cathodes was observed for composite cathodes, produced by mixing powders of YSZ and LSM, and this result was explained by the contribution of triple-phase boundaries (TPB) length of electrode/electrolyte/gas interface. It is clear that composite electrodes (i.e., LSM-YSZ) perform much well than the single component electrodes (i.e., LSM). However, there still remain controversies on the details of the electrode kinetics, since the experi-

†E-mail: leeyk@mail.uiduk.ac.kr

mental conditions (i.e., chemical composition, grain/particle size distribution, microstructure, thickness, firing temperature, porosity, etc.) play an important role. Therefore, more information is needed to understand the performance of thin-film SOFCs with LSM-YSZ composite electrodes at reduced temperatures.

In this study the electrochemical evaluation of a series of perovskite electrodes is presented. Specifically, composite cathodes of 50/50 vol% LSM-YSZ are evaluated for use in conventional and thin-film SOFCs.

2. Experimental

For the electrolytes, sintered 8 mol% YSZ pellets were used. YSZ powder supplied by Tosoh Co., Ltd. was pressed and sintered in air at 1450°C for 4 h into pellets of ca. 30 mm in diameter and ca. 0.6 mm in thickness with relative density of more than 95%. And then YSZ pellets were made curved surface intentionally for the protection of surface contamination from alumina plates and the reduction of cathode firing process by aerosol spray deposition of both surfaces.

Various $La_{1-x}Sr_xMnO_3$ (LSM) powder with $0 \leq x \leq 0.5$ were prepared at a glycine/nitrate ratio of 0.5 by the glycine-nitrate combustion process,[8] and then calcined in air at 1200 °C for 4 h. The resulting LSM powders and YSZ powders calcined at same condition were milled for 1.5 h in acetone using zirconia media in a ratio 50/50 vol%. The LSM-YSZ cathode powders were dried and then dispersed in isopropyl alcohol and applied to a 1 cm × 1 cm masked off area on the electrolyte plates as a working electrode, and fired at 1100°C for 4 h. The Pt counter and Pt reference electrodes were deposited on the other side of the YSZ plates by a thin layer of Pt paste from Heraeus, and then fired at 950°C for 0.5 h. The current collector was Pt mesh fixed to the electrode surface by Pt paste, followed by firing at 950°C for 0.5 h, and then the Pt mesh was well adhered to the surface of the electrodes. The thickness of the working electrode (LSM-YSZ) was measured about 10 μm by SEM. Also, the cells with YSZ electrolyte sandwiched between two like cathode materials consisting of LSM-YSZ were prepared.

IS was used to measure the electrode resistivity of the LSM-YSZ cathode layers on YSZ electrolytes using a computer-controlled Solatron SI 1260 Impedance/Gain-Phase Analyzer and Potentiostat/Galvanostat. Impedance spectra were taken in the frequency range of 0.1 Hz to 100 kHz, and the applied AC amplitude was set to 10 mV.

3. Results and Discussion

Fig. 1 shows the temperature-dependent impedance spectra of $La_{0.85}Sr_{0.15}MnO_3$-YSZ (LSM15-YSZ)/YSZ interface which were obtained under increasing and decreasing an operated temperature in the range of 700 to 900°C. In the figure, the 1 and 2 represent measured results under increasing and decreasing of temperature, respectively, within 1 day, and 3 and 4 without 1 day after first measurement. These spectra clearly indicate that the interfacial impedance (or polarization

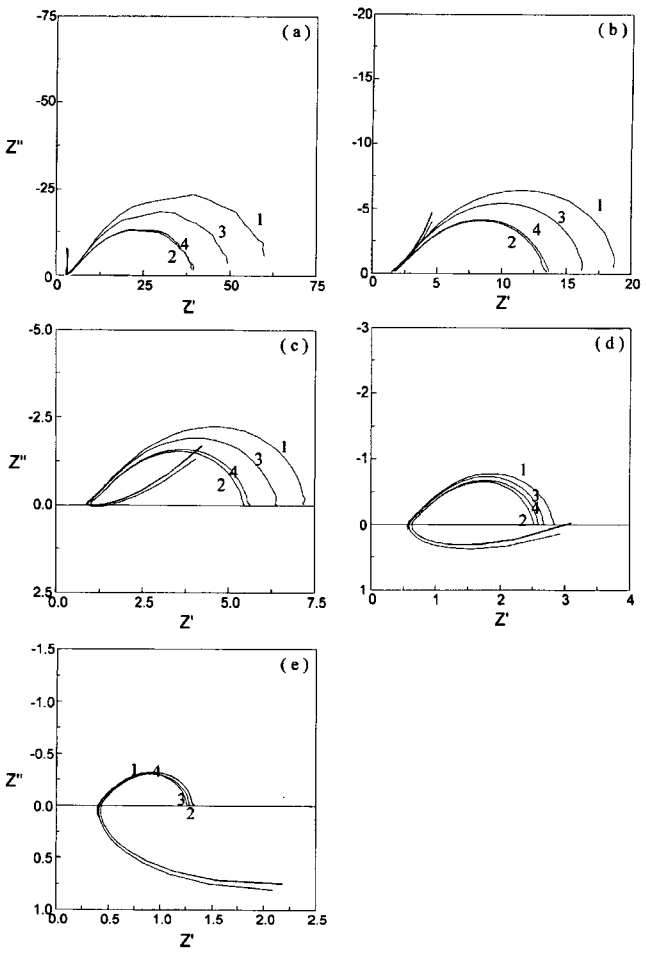

Fig. 1. Evolution of the impedance spectra for a LSM15-YSZ cathode on YSZ measured at (a) 700°C, (b) 750°C, (c) 800°C, (d) 850°C and (e) 900°C in air. In each figure, the 1 and 2 represent measured plots under increasing and decreasing of temperature, respectively, within 1 day, and 3 and 4 without 1 day after first measurement.

resistance) is a strong function of operating temperature. With increasing operating temperature the LSM15-YSZ cathode resistance decreases. The impedance spectra also present a discrepancy between spectra obtained under increasing and decreasing of operated temperature in the range of 700 to 900°C dependent of operation time except 900°C. This discrepancy of polarization resistance (arc size) is interpreted by the formation of oxygen vacancies or oxygen nonstoichiometry in the LSM-YSZ electrode.[9-12] Therefore, the stable conditions for LSM-YSZ/YSZ cells are typically reached at 900°C, and not reached within 2 days at below 900°C of operation. Also, impedance spectra typically show an induction effect at high frequencies originating from Pt lead connections and instrumentation.

Fig. 2 shows deconvolution of the impedance spectrum of LSM15-YSZ cathode measured at 900°C in air with the equivalent circuit after subtraction of the induction. Deconvolution of the obtained complex impedance spectrum was performed with Zplot and Zview (Scribner Associates Inc.) electrochemical impedance software, and parameters of the appropriate equivalent circuit model was determined. The

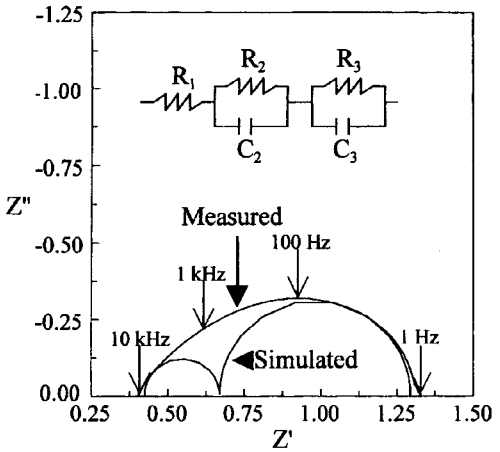

Fig. 2. Deconvolution of the impedance spectrum of LSM15-YSZ cathode measured at 900°C in air with the equivalent circuit after subtraction of the inductance (R_1: YSZ electrolyte resistance, R_2: charge transfer resistance, R_3: mass transfer resistance, C_2, C_3: distributed capacitances).

observed impedance spectrum of the LSM-YSZ electrode shows overlapping of two semicircles: the one at the high frequency side was due to charge transfer process; the other at the low frequency side was due to mass transfer process (or diffusion process) of oxide ion.[13-19] Also, the spectrum shows that high frequency arc is much smaller than the low frequency arc, and there is a 45° slope at high frequency end, indicating a Warburg impedance. This result indicates that the mass transfer process (low frequency arc) is dominant in LSM-YSZ cathode.

Fig. 3 shows the impedance spectra obtained from LSM15-YSZ and LSM15 cathodes deposited on as-sintered YSZ surface and sanded YSZ surface exposed to air at 800°C. The polarization resistance of LSM15-YSZ and LSM15 deposited on sanded YSZ surface typically decreased compared to those of as-sintered YSZ surface. This result related to the effective TPB length and surface impurities. A sintered YSZ surface is generally smooth and glossy and contains surface impurities such as silica and alumina. Therefore, the surface treatment such as polishing and etching is helpful to the creation of extra TPB in addition to the removal of surface impurities. If the impurities are present at the electrode/electrolyte triple phase boundary interface, then cleary it can restrict the flux of oxygen ions into the electrolyte. The removal of impurities, exceptionally silica, in YSZ electrolytes can thus decrease the electrode resistivity as well as the ionic resistivity in the YSZ electrolyte. The surface pretreatment also helps increase the adhesion of added electrode materials during further processing. Other researchers also have reported similar results.[20,21]

In Fig. 3, the polarization resistance of LSM15-YSZ cathode is thus lower than that of LSM15. This result indicates that with addition of YSZ to the LSM15 electrode, the spatial enlargement of the TPB length was realized so that the oxygen ion transfer step could be accelerated. Also, one thing to note from Fig. 3 is that the polarization resistance of LSM15-YSZ cathode deposited on sanded YSZ surface was much reduced compared to that of LSM15. From this result, it was believed that the polarization resistance of LSM15-YSZ cathode deposited on sanded YSZ surface drastically decreased due to the combination of spatial enlargement of the TPB length and removal of the surface impurities as mentioned above.

Fig. 4 shows the impedance spectra obtained from LSM15-YSZ and LSM15 with and without Ni or Sr catalytic interlayer coating between cathode and electrolyte. For LSM15-YSZ with a catalytic interlayer (Ni or Sr), the polarization resistance was much smaller than LSM15-YSZ without a catalytic interlayer, whereas for the LSM15 with a catalytic interlayer, the opposite result was obtained. We cannot exactly explain the difference at present. Generally, polariz-

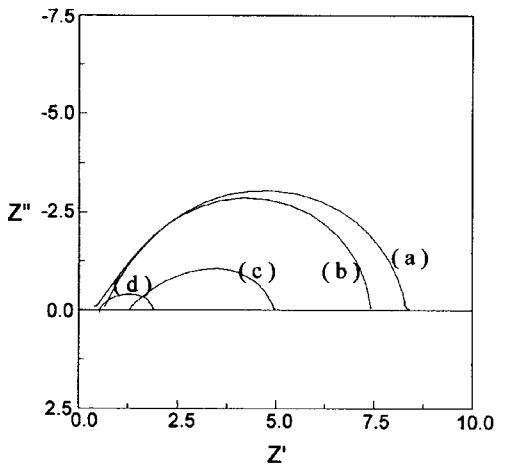

Fig. 3. Impedance spectra for the LSM15/YSZ and LSM15-YSZ/YSZ electrodes with different YSZ electrolyte surfaces at 800°C in air; (a) LSM15 with as-sintered YSZ surface, (b) LSM15 with sanded YSZ surface, (c) LSM15-YSZ with as-sintered YSZ surface and (d) LSM15-YSZ with sanded YSZ surface.

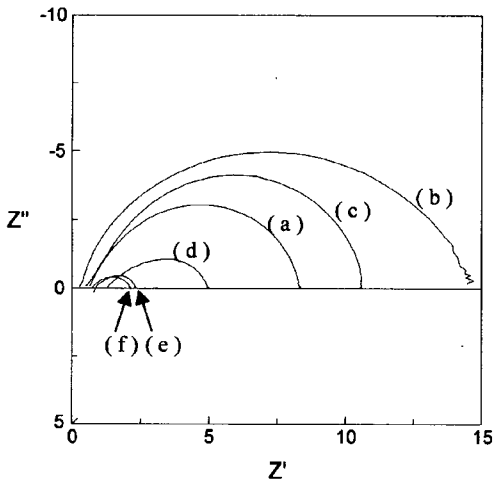

Fig. 4. Impedance spectra for the LSM15/YSZ and LSM15-YSZ/YSZ electrodes with different catalytic interlayer at 800°C in air; (a) LSM15 with no catalytic interlayer, (b) LSM15 with Ni-nitrate, (c) LSM15 with Sr-nitrate, (d) LSM15-YSZ with no catalytic interlayer, (e) LSM15-YSZ with Ni-nitrate and (f) LSM15-YSZ with Sr-nitrate.

ability of SOFC electrodes diminishes by percolation of catalytically active elements into surface layers of the solid electrolyte. And then the effect of catalytic interlayer is associated with an increasing rate of interface oxygen exchange at either electrode/gas or electrolyte/gas surfaces, with an increasing TPB activity, or with a combination of these factors. But we analogize that substitution of manganese by diffusion and/or reaction of catalytic element into the LSM15 leads to a large decrease in oxygen permeability of the LSM15, though it allows an increase in the electrochemical activity of the LSM15 cathode. These results also indicate that a uniform coating of Ni or Sr throughout the YSZ surface is not advisable, although the LSM15-YSZ cell showed much better polarization resistance characteristics compared to a cell fabricated with Ni- or Sr-free YSZ. The precise analysis will be made in future work.

Fig. 5 shows typical impedance spectra of LSM-YSZ/YSZ /LSM-YSZ cells with different LSM-YSZ electrode compositions on YSZ electrolyte exposed to air at 900°C. Note that the spectra of the cathodic side half-cell and anodic side half-cell were not actually taken from the same half-cell owing to geometrical asymmetry (curved surface) of the two half-cell. These spectra clearly indicate that the interfacial impedance is a strong function of the composition of electrode materials and the geometry of electrolytes. But these spectra don't present a tendency with increasing the Sr-content in LSM-YSZ. The interfacial impedance of LSM-YSZ electrodes with different Sr-content seems to be related to electrochemical activity, ionic diffusion and quality of the contact with electrolyte due to the difference in ionic radii between La and Sr, the number of vacancies in La(Sr) sites, adhesion of the LSM-YSZ electrode to the YSZ electrolyte etc. Therefore, at this time we suspect that the composition of the LSM in LSM-YSZ electrode is not as important as the bonding of the YSZ in electrode to the YSZ in the electrolyte or as important as the vol% of the YSZ in the electrode. This will be confirmed via future study.

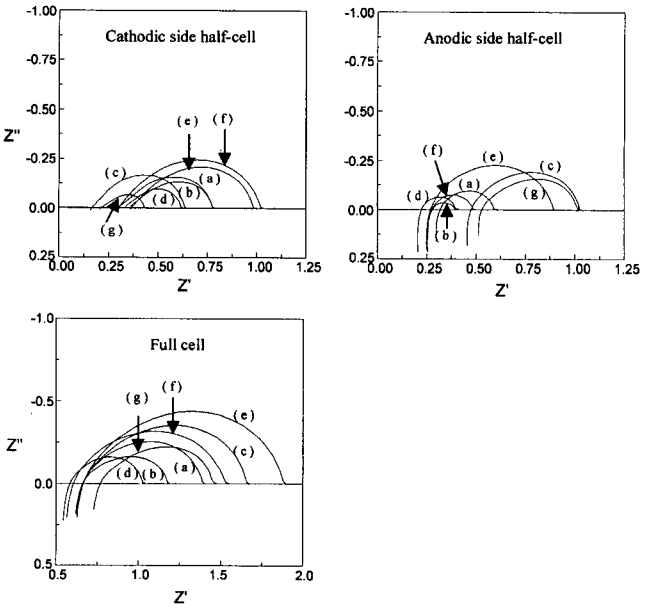

Fig. 5. Impedance spectra for the LSM-YSZ/YSZ/LSM-YSZ cells under various cathode compositions at 900°C in air; (a) $LaMnO_3$-YSZ, (b) $La_{0.9}Sr_{0.1}MnO_3$-YSZ, (c) $La_{0.85}Sr_{0.15}MnO_3$-YSZ, (d) $La_{0.8}Sr_{0.2}MnO_3$-YSZ, (e) $La_{0.7}Sr_{0.3}MnO_3$-YSZ, (f) $La_{0.6}Sr_{0.4}MnO_3$-YSZ and (g) $La_{0.5}Sr_{0.5}MnO_3$-YSZ.

Fig. 6 shows impedance spectra obtained from LSM15-YSZ/YSZ/Pt cells with two different types of Pt anodes ((a) Pt-1 and (b) Pt-2). The two Pt pastes also applied as an adhesive of current collector in two electrodes. These spectra in anodic side half-cell clearly indicate that the interfacial impedance is a strong function of the formulation of the Pt pastes. In addition, polarization resistance of anodic side with Pt-1 paste is much smaller than that of anodic side with Pt-2 paste. Also, interfacial impedance of cathodic side half-cell affected strongly owing to the change in the microstructure by Pt pastes applied as an adhesive of current collector. Furthermore, the impedance plot of cathodic side with the Pt-2 paste at low frequency shows a diffusion tail. Therefore, use of the only one batch pt paste is advisable for acquisition of consistent data.

Fig. 7 shows the impedance spectra of LSM-YSZ/YSZ/Pt cell with LSM15-YSZ cathodes deposited on curved YSZ surface in air at 900°C. The LSM-YSZ cathode and Pt anode

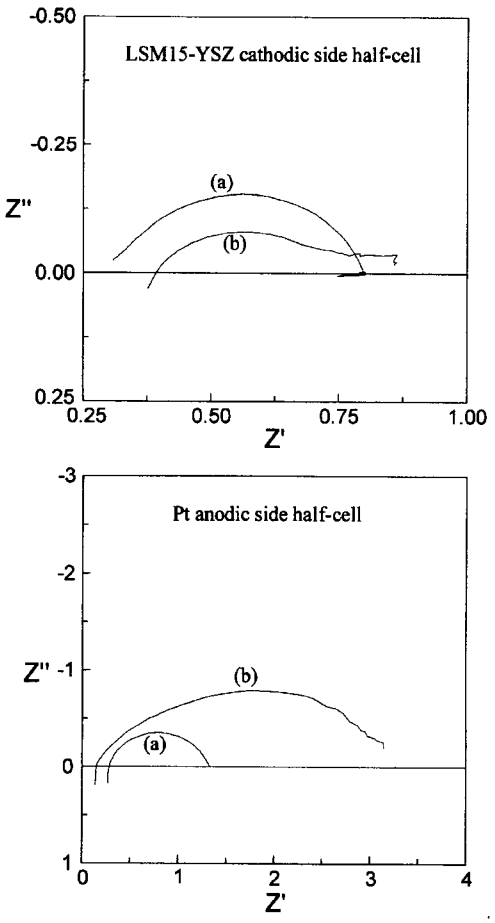

Fig. 6. Impedance spectra obtained from LSM15-YSZ/YSZ/Pt cells with two different types of Pt anodes ((a) Pt-1 and (b) Pt-2). The two Pt pastes also applied as an adhesive of current collector in two electrodes.

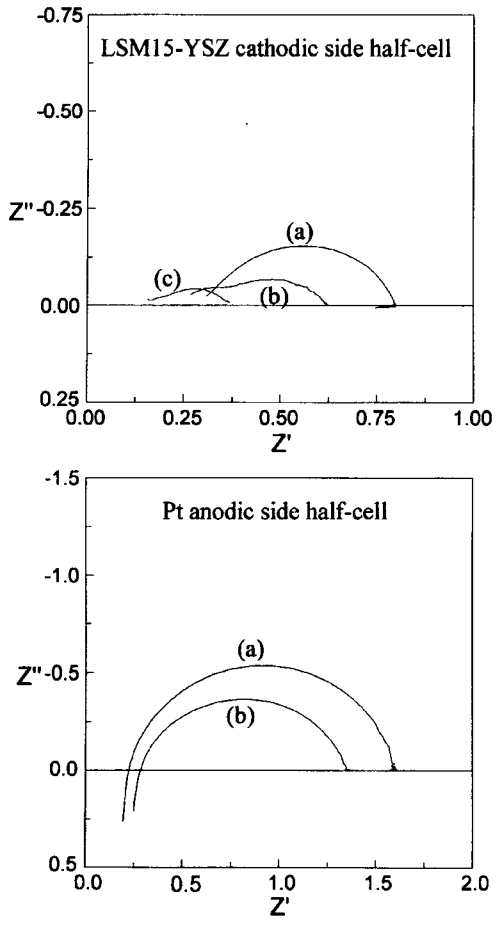

Fig. 7. Impedance spectra of LSM15-YSZ cathodes with different YSZ electrolyte geometry at 900°C in air; (a) electrode deposited on convex YSZ surface, (b) electrode deposited on concave YSZ surface and (c) electrode deposited on flat YSZ surface.

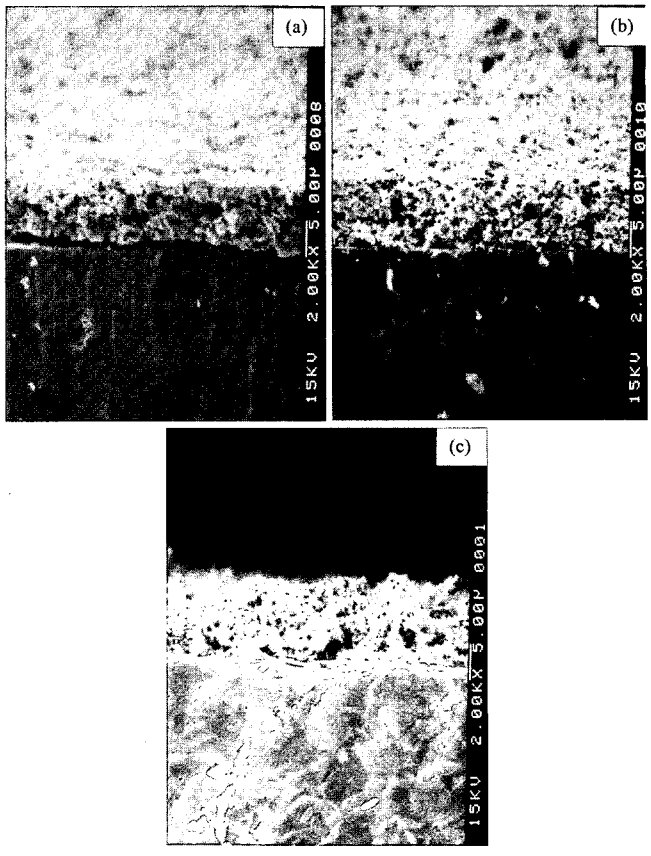

Fig. 8. SEM photograph of a cross-sectional fracture surface of LSM15-YSZ electrodes on (a) convex, (b) concave and (c) flat YSZ plates.

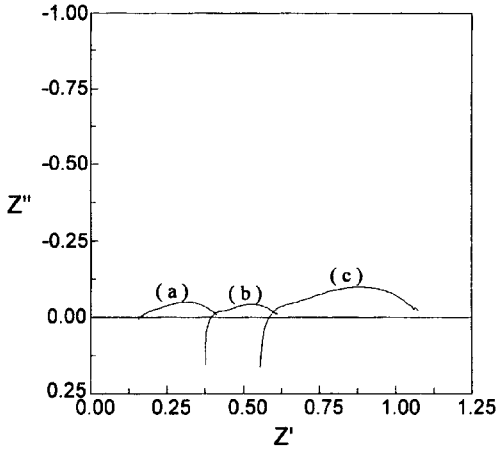

Fig. 9. Impedance spectra obtain from LSM15-YSZ/YSZ/LSM15-YSZ cell deposited on flat YSZ plate: (a) cathodic side half-cell, (b) anodic side half-cell and (c) full cell. The Pt paste used was changed.

deposited on concave side of YSZ plates showed lower resistivity than those of convex side, and the LSM-YSZ cathode deposited on concave side also showed lower resistivity compared to that of flat YSZ plate. These results are caused by concentration polarization due to the contact in electrode/electrolyte interface and the TPB length shown in SEM images of Fig. 8; the direct penetration of oxygen into the electrode/electrolyte interface and the TPB length will be delayed in YSZ plates with curved surface due to the poor contact and small TPB length. Therefore, use of electrolyte with flat surface is advisable for fabrication of high performance cell.

Fig. 8 shows the cross-section SEM photographs of three LSM-YSZ cathode layers. The electrode/electrolyte contact of convex side in the LSM-YSZ electrode is much worse with comparatively less TPB length compared to those of concave and flat side. Also, the SEM image clearly shows that the porous LSM15-YSZ structure has a thickness of about 10 μm, and it is impossible to distinguish between the LSM and YSZ particles in LSM-YSZ layer.

Fig. 9 shows impedance spectra obtained from LSM15-YSZ/YSZ/LSM15-YSZ cell deposited on flat YSZ plate. The high frequency intercept does not approach zero owing to resistance of electrolyte and measuring leads. These spectra also present a consistency in interfacial impedance of cathodic side and anodic side half-cell, while the spectra present a discrepancy in ohmic polarization of YSZ electrolyte. The discrepancy is interpreted by effect of reference electrode position on impedance testing. When the anode and cathode were attached to the electrolyte symmetrically, and the reference electrode was far from both working and counter electrodes, accurate polarization resistance against a reference

electrode can be measured.[22] Therefore, this discrepancy could be solved moving the reference electrode further away.

Fig. 10 shows impedance spectra of LSM-YSZ cathodes before and after passing a current of 1 A/cm^2. Measurements were taken at 900°C, before (a), 4 min after (b), and 24 h after (c) passing a current of 1 A/cm^2 for 24 h. At the impedances measured 4 min after switching off the current, a decrease of the electrode resistance in a few cells ($LaMnO_3$-YSZ, $La_{0.9}Sr_{0.1}MnO_3$-YSZ, and $La_{0.8}Sr_{0.2}MnO_3$-YSZ) among cells with different cathode compositions was observed compared with those before current passage, whereas at the impedances measured 24 h after switching off the current, a drastic increase of the electrode resistance was observed in all cells except cell with $La_{0.8}Sr_{0.2}MnO_3$-YSZ cathode. These observed phenomena are caused by change in the microstructure before and after current passage. Therefore, we recommend $La_{0.8}Sr_{0.2}MnO_3$-YSZ cathode with relatively low electrode resistance before and after current passage as a most promising cathode material in present work.

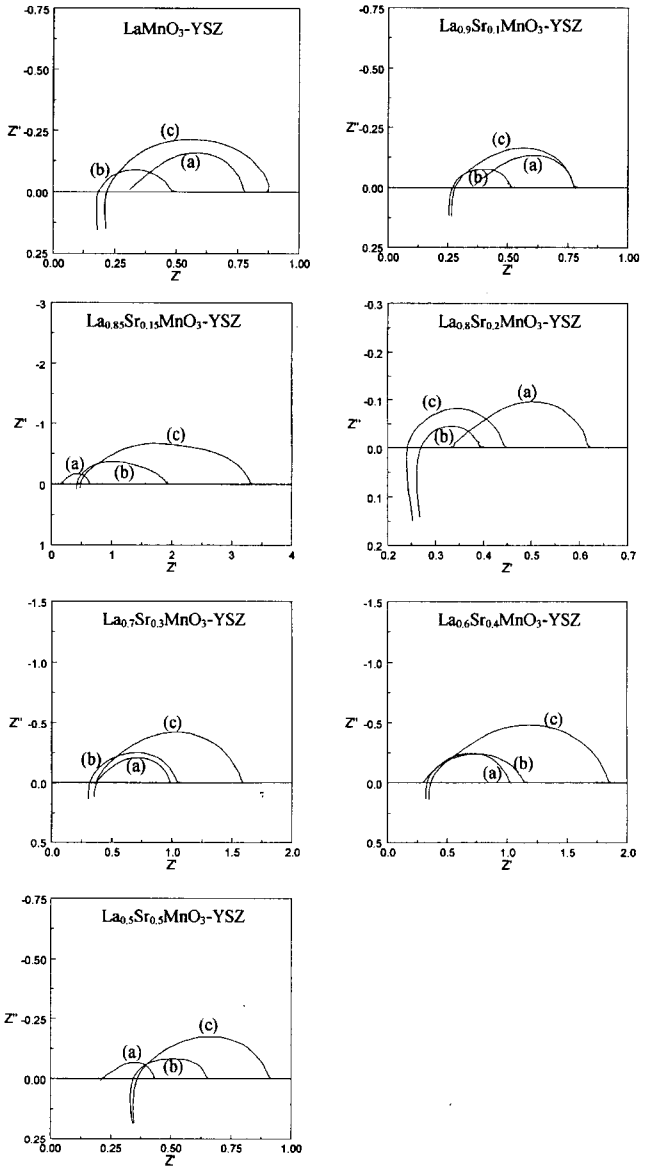

Fig. 10. Impedance spectra of LSM-YSZ cathodes before and after passing a current of 1 A/cm^2. Measurements were taken at 900°C, (a) before, (b) 4 min after and (c) 24 h after passing a current of 1 A/cm^2 for 24 h.

Fig. 11 and 12 show SEM photographs of $La_{0.85}Sr_{0.15}MnO_3$-YSZ (LSM15-YSZ) and $La_{0.8}Sr_{0.2}MnO_3$-YSZ (LSM20-YSZ) in LSM-YSZ/YSZ/LSM-YSZ cells before and after passing a current of 1 A/cm^2, respectively. The difference in the thickness of LSM-YSZ is due to the detachment of a part of LSM-YSZ with removal of Pt mesh (current collector) from LSM-YSZ/YSZ cell for SEM observation. In the present work, we were not able to detect any change in the microstructure of the cathodic side in LSM-YSZ specimens induced by current passage. But, the SEM images clearly show that a new phase was formed at the interface between YSZ and LSM-YSZ of the anodic side after current passage. This means that the components of the LSM-YSZ diffuse into the YSZ after current passage. Also, LSM15-YSZ side of coupled LSM15-YSZ/YSZ anodic side after current passage has enhanced grain growth and sinterability compared to that before current passage, whereas the LSM20-YSZ side doesn't show a change in microstructure before and after current passage. The enhanced grain growth and sinterability led to inhomogeneous and dense microstructure resulting in higher electrode polarization in LSM15-YSZ side. We con-

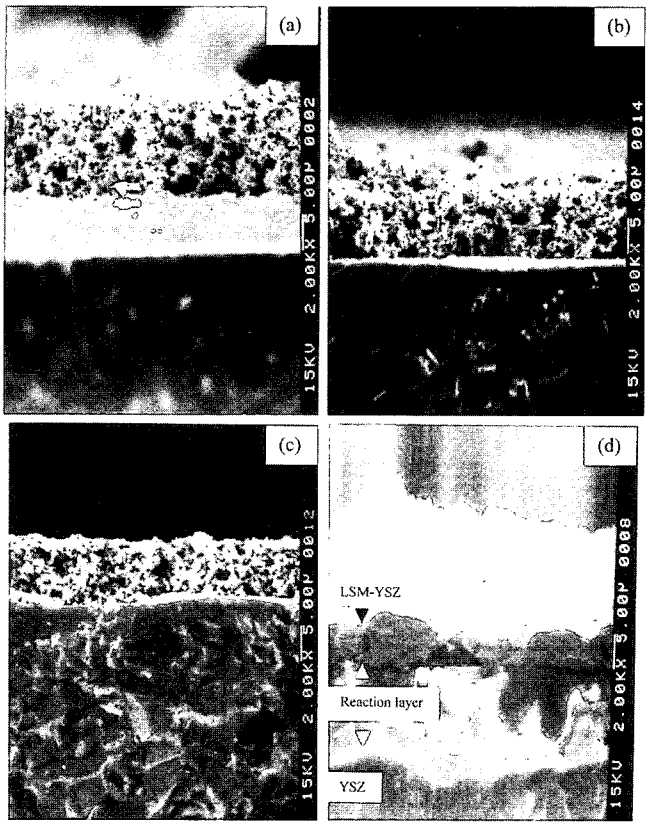

Fig. 11. SEM photographs of a cross-sectional fracture surface of LSM15-YSZ electrodes before and after current passage; (a) cathodic side before current passage, (b) anodic side before current passage, (c) cathodic side after current passage and (d) anodic side after current passage.

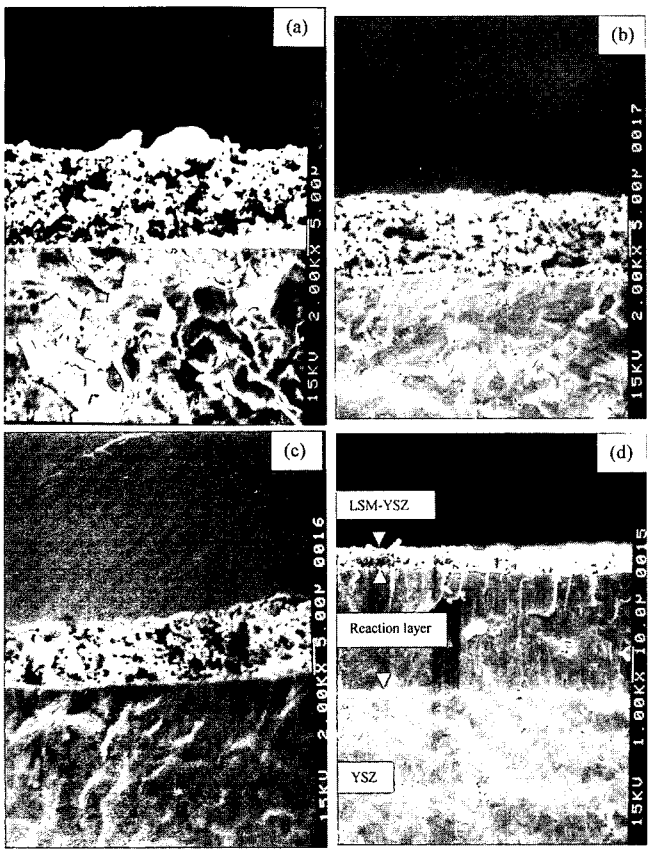

Fig. 12. SEM photographs of a cross-sectional fracture surface of LSM20-YSZ electrodes before and after current passage; (a) cathodic side before current passage, (b) anodic side before current passage, (c) cathodic side after current passage and (d) anodic side after current passage.

sider that these changes in microstructure (morphology) resulted in the change of impedance before and after current passage for various electrode compositions. The exact analysis for these differences will be left for future work. In fact, the formation of new reaction layer in LSM-YSZ/YSZ anodic side is not desirable for the fabrication of long-term stable SOFC systems although the case of LSM20-YSZ after current passage showed much smaller polarization resistance characteristics compared with that before current passage. To solve these problems, the followings are suggested: (1) coating the YSZ surfaces in anodic sides of the component layers with an inactive substance: (2) making a anodic side inactive to SOFC components by replacing the anode material such as Pt, Ni-YSZ, etc.

4. Conclusions

The cathode resistivities of 50/50 vol% LSM-YSZ for use in conventional and thin-film SOFCs were investigated by the complex ac impedance measurement. Further improvements of electrochemical performance for LSM-YSZ cathode materials at reduced temperatures may come from engineering of electrolyte/electrode interface, i.e. the electrochemically active layer and polished flat electrolyte surface. The impedance response was very sensitive to fabrication origin of the LSM-YSZ/YSZ cells, and reproducible impedance spectra could be obtained by establishing very consistent process and test procedures of the cell components. The results obtained indicate that some of the conditions can be of great importance for the properties of the cathode and thus the performance of the SOFC.

Acknowledgment

One of the authors, You-Kee Lee, wishes to thank KOSEF (Korea Science and Engineering Foundation) for a Post Doctoral Fellowship.

References

1. L. S. Wang and S. A. Barnett, *Solid State Ionics*, **61**, 273 (1993).
2. T. W. Kueper, S. J. Visco and L. C. De Jonghe, *ibid.*, **52**, 251 (1992).
3. H. Fukunaga, M. Ihara, K. Sakaki and K. Yamada, *ibid.*, **86-88**, 1179 (1996).
4. P. K. Srivastava, T. Quach, Y. Y. Duan, R. Donelson, S. P. Jiang, F. T. Ciacchi and S. P. S. Badwal, *ibid.*, **99**, 311 (1997).
5. S. Souza, S. J. Visco and L. C. De Jonghe, *ibid.*, **98**, 57 (1997).
6. T. Ioroi, T. Hara, Y. Uchimoto, Z. Ogumi and Z. Takehara, *J. Electrochem. Soc.*, **144**, 1362 (1997).
7. N. Q. Minh, *J. Am. Ceram. Soc.*, **76**, 563 (1993).
8. L. A. Chick, L. R. Pederson, G. D. Maupin, J. L. Bates, L. E. Thomas and G. J. Exarhos, *Mat. Lett.*, **10**, 6 (1990).
9. M. J. L. Østergård and M. Mogensen, *Electrochem. Acta*, **38**, 2105 (1993).
10. H. Y. Lee, W. S. Cho, S. M. Oh, H-D. Wiemh fer and W. Göpel, *J. Electrochem. Soc.*, **142**, 2659 (1995).
11. Y. Jiang, S. Wang, Y. Zhang, J. Yan and W. Li, *ibid.*, **145**, 373 (1998).
12. A. Hammouche, E. Siebert, A. Hammon, M. Kleitz and A. Caneiro, *ibid.*, **138**, 1212 (1991).
13. A. Hahn and H. Landes, Proceedings 5th Intern. Symp. SOFC, Archen, Germany, June 1997, U. Stimming, S. C. Singhal, H. Tagawa, W. Lehnert eds., p.595, The Electrochemical Society, Inc., Pennington, NJ.
14. Y. Shibuya and H. Nagamoto, *ibid.*, p. 510.
15. T. Ioroi, T. Hara, Y. Uchimoto, Z. Ogumi and Z. Takehara, *J. Electrochem. Soc.*, **145**, 1999 (1998).
16. E. Siebert, A. Hammouche and M. Kleitz, *Electrochem. Acta*, **40**, 1741 (1995).
17. M. J. L. Østergård, C. Clausen, C. Bagger and M. Mogensen, *Electrochem. Acta*, **40**, 1971 (1995).
18. E. P. Murray, T. Tsai and S. A. Barnett, 1998 Fuel Cell Seminar Abstracts, p. 414.
19. M. Juhl, S. Primdahl and M. Mogensen, Proc. 17th Risø Intern. Symp. on Mat. Sci., F. W. Poulsen, N. Bonanos, S. Linderoth, M. Mogensen and B. Zachau-Christiansen eds., Risø National Laboratory, Denmark, p. 295 (1996).
20. T. Tsai and S. A. Barnett, *J. Electrochem. Soc.*, **145**, 1696 (1998).
21. J-M. Bae and B. C. H. Steele, *Solid State Ionics*, **106**, 247 (1998).
22. M. Nagata, Y. Itoh and H. Iwahara, *ibid.*, **67**, 215 (1994).